



ELSEVIER

Journal of Alloys and Compounds 317–318 (2001) 525–531

Journal of
ALLOYS
AND COMPOUNDS

www.elsevier.com/locate/jallcom

Thermodynamic stabilities of intermediate phases in the Ca–Si system

S. Brutti^a, A. Ciccioni^a, G. Balducci^{a,*}, G. Gigli^a, P. Manfrinetti^b, M. Napoletano^b^aDipartimento di Chimica, Università di Roma La Sapienza, p.le A. Moro 5, I-00185, Roma, Italy^bDipartimento di Chimica e Chimica Industriale, Università di Genova, via Dodecaneso 31, I-16146, Genova, Italy

Abstract

Vaporization thermodynamics in the binary system calcium–silicon has been studied by Knudsen effusion-mass spectrometry and vacuum microbalance techniques. The equilibrium partial pressure of Ca(g) over the two-phase regions in the composition range 20–75at.% Si has been measured and the standard enthalpy changes for the appropriate vaporization reactions were determined from the temperature dependence of the measured vapor pressures. The standard reaction enthalpy changes were also evaluated by the third-law method using the pressure data in conjunction with estimated Gibbs energy functions. Standard enthalpies of formation of the calcium silicides were derived from the standard reaction enthalpy values at room temperature. The results obtained for $\Delta_f H^\circ_{298}$ were the following: $\text{Ca}_2\text{Si} = -56.1 \pm 3.1$, $\text{Ca}_5\text{Si}_3 = -55.3 \pm 3.5$, $\text{CaSi} = -49.6 \pm 2.2$, $\text{Ca}_3\text{Si}_4 = -40.6 \pm 1.5$, $\text{Ca}_{14}\text{Si}_{19} = -44.4 \pm 2.3$, $\text{CaSi}_2 = -37.8 \pm 1.6$ all in kJ/mol atoms. The results for Ca_2Si , CaSi and CaSi_2 may be compared with previous measurements, all other results are first determinations. © 2001 Elsevier Science B.V. All rights reserved.

Keywords: Calcium silicides; Intermetallics; Thermodynamic and thermochemical properties; Heats of formation; Vaporization behaviour; Knudsen effusion-mass spectrometry

1. Introduction

Although the Ca–Si system has been in the past the object of several investigations, mainly concerning the phase diagram, many uncertainties remained until recently in the liquidus curves and invariant temperatures as well as in the number and identity of the intermediate phases. Therefore the published phase diagram in current compilation [1] of the whole system cannot be considered as definitive. The available data of the thermodynamic properties of the intermediate phases are rather scarce and controversial.

Kubaschewski and Villa [2] determined calorimetrically in an early study the heats of formation of the three solid silicides Ca_2Si , CaSi and CaSi_2 . Apart from a subsequent work from Shchukarev et al. [3] limited to the Ca_2Si compound, these data apparently remain the only calorimetric results on Ca–Si alloys. Wynnyckyj et al. in two papers [4,5] reported on the measurement of calcium vapor pressure over a few calcium–silicon alloys mainly in the silicon rich side of the phase diagram (50–76at.% Si) and in the liquidus domain, and calculated the components activity. However, due to the incomplete knowledge of the

phase diagram a correct attribution of vapor pressures to well defined two-phase equilibria appears questionable. A similar argument applies to the previous effusion data by Muradov et al. [6]. Finally, emf measurements on the CaSi_2 phase were reported [7]. On the basis of phase diagram and thermodynamic information at the time available, Anglezio et al. assessed the whole system by using the Calphad approach [8].

In view of the renewed interest in the calcium silicides, due to the electronic and superconductive properties of some of these compounds which make them potentially attractive in materials applications, recently a great deal of research has been carried out mainly on the physical properties, but also in crystal chemistry and low-temperature thermodynamic properties.

Manfrinetti et al. [9] recently reinvestigated the Ca–Si phase diagram in the composition range 0–75at.% Si (Fig. 1). They confirmed the existence of five intermediate phases and characterized for the first time a new compound, the Zintl-phase Ca_3Si_4 . Affronte et al. [10] measured the low temperature heat capacities and resistivities for CaSi and CaSi_2 . Canepa et al. [11] measured by adiabatic calorimetry the heat capacities in the temperature range 3–300 K for three silicon-rich Ca–Si compounds (Ca_3Si_4 , $\text{Ca}_{14}\text{Si}_{19}$, CaSi_2). They calculated the thermodynamic functions at 298 K and subsequently extended

*Corresponding author.

E-mail address: balducci@axcasp.caspur.it (G. Balducci).

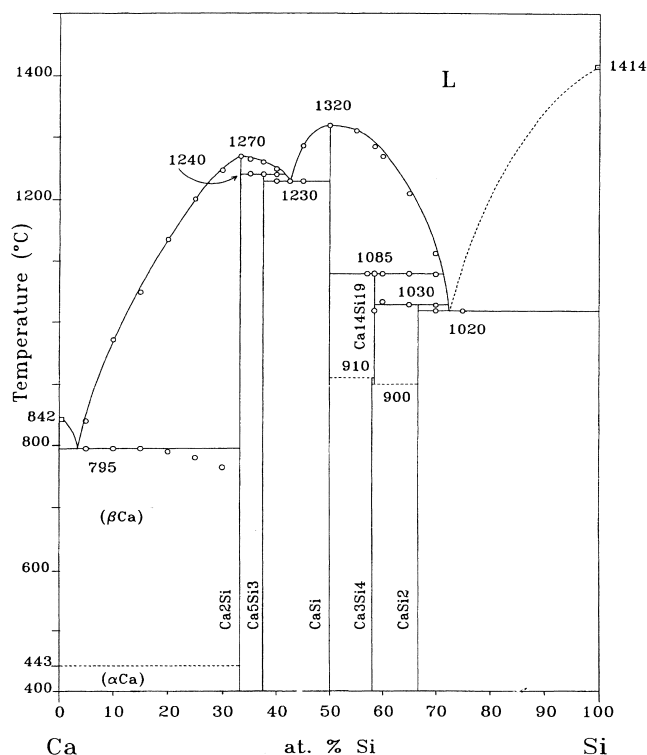


Fig. 1. Ca–Si phase diagram after Manfrinetti et al. [9].

these measurement to the other compounds of the same system [12].

On the whole, accurate thermodynamic data are rather scarce or lacking, in particular high temperature free energy data for the formation of the Ca–Si compounds. On the other hand these data are required in phase diagram optimization and in modeling deposition processes using a free energy minimization approach.

In the present paper we report the results of high temperature vaporization experiments carried out on several Ca–Si alloys in the composition range 20–75 at.% Si.

From the temperature dependence of the vapor pressure values measured over a single phase or two-phase mixtures the enthalpy changes for the decomposition reactions were determined and hence the standard enthalpies of formation for the various calcium silicides present in the phase diagram [9], were derived.

2. Experimental

2.1. Sample preparation and characterization

Calcium–silicon alloys were prepared by melting elemental calcium (purity 99.5 wt%) and silicon (purity 99.999 wt%) in closed containers due to the much higher vapor pressure of calcium compared to silicon. Weighted amounts of the two elements in form of small Ca chips and Si powder were pressed into pellets and then molten in an induction furnace in tantalum crucibles closed by arc

welding. The samples were annealed in sealed quartz tubes under vacuum and then characterized by X-ray diffraction. The composition of some of them were also checked by electron probe microanalysis (EPMA). In most cases the vaporization residues (see subsequent section) were also subjected to this analysis procedure.

2.2. Vapor pressure measurement

Vaporization experiments were mainly performed using a Nuclide model 12-60 HT single focusing magnetic sector mass spectrometer coupled with a Knudsen cell assembly. The effusion cells consisted of tantalum or molybdenum cells with cylindrical effusion orifices of 1.0 mm or 0.5 mm in diameter which were inserted in an outer molybdenum crucible. The non-ideality of the effusion orifice was accounted for in the subsequent calibration procedure for converting ion intensities into pressures.

The cell was heated with a tungsten resistance heater. Temperatures were measured with a disappearing-filament optical pyrometer by sighting into a blackbody cavity in the bottom of the crucible. In a few experiments temperatures were also measured with a calibrated Pt–Pt(10% Rh) thermocouple placed in tight contact with the bottom of the crucible. In a preliminary experiment the vapors effusing from the Knudsen cell were ionized using an electron energy of 70 eV and a total emission current of 1 mA. Only monoatomic Ca(g) was detected in the vapor at the temperature of the measurement. This was confirmed in all subsequent experiments. At 70 eV the positive ions formed by electron impact were Ca⁺ and Ca²⁺, the contribution of the double ionized calcium being 10–15% of the Ca⁺ intensity. As the ionization efficiency curves showed a maximum between 25 and 30 eV we choose to perform all the subsequent intensity measurements at an operating electron energy of 25 eV, practically below the threshold of the second ionization potential of Ca.

In a KC–MS experiment the partial pressure of the species *i*, in this case Ca(g), is related to the measured ion current I_i^+ by the relation:

$$p_i = k_{\text{str}} f_i I_i^+ T \quad (1a)$$

where k_{str} is the instrumental constant, the factor $f_i = 1/(\sigma_i \gamma_i a_i)$ includes the electron impact cross section (σ_i), the multiplier gain (γ_i), and the isotopic abundance (a_i) of the specific ion. The determination of k_{str} was performed repeatedly by vaporization of a standard substance such as high purity elemental silver and comparing its intensity versus temperature (including the melting temperature) to the reference vapor pressure data for silver [13]. Further checks of the calibration constant were made by studying the dissociation equilibrium $\text{Ag}_2 = 2\text{Ag}$ for which the ΔH°_0 is well established.

Some vaporization runs, in particular for Ca-rich compositions, were also performed with a vacuum microbal-

ance to the arm of which was suspended an effusion cell identical in material and geometry to that used in the KC–MS experiments. In the Knudsen effusion-weight loss (KC–WL) experiments the partial vapor pressure of the species i is given by the relation:

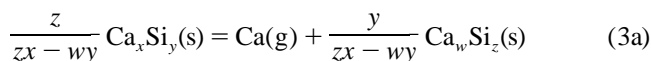
$$p_i = \frac{dm_i}{A_0 dt} \sqrt{\frac{2\pi RT}{M_i}} \quad (2a)$$

were A_0 is the area of the effusion orifice, M_i is the molecular weight of the effusion species and dm_i/dt is the weight-loss rate.

3. Results and discussion

3.1. Thermodynamic calculations

In the composition range 20–75at.% Si, Ca(g) was the only species detected in the vapor phase. The decomposition equilibrium can then be written (by mole of gas) in the form:



where Ca_xSi_y and Ca_zSi_w are two intermediate phases contiguous in the phase diagram. Apparently no accurate solid solubility data for this system are available in the literature. However, solubility in both the Ca-rich and Si-rich terminal regions is likely to be very small. The vaporization processes in these regions can then be described with good approximation by Eq. (3a) with $x=1$, $y=0$ (Ca-rich end: vaporization of pure calcium) and $x=z=1$, $y=2$, $w=0$ (Si-rich end: decomposition of CaSi_2 to pure silicon), respectively. Therefore, by assuming negligible solid solubility and considering that all the intermediate phases are of fixed composition, the equilibrium constant for all the decomposition reactions is given by:

$$K = p_{\text{Ca}}/\text{bar} \quad (4a)$$

where p_{Ca} is expressed in bar. By measuring p_{Ca} over equilibrated two-phases mixtures as a function of temperature is then possible to derive the enthalpy changes for the relevant reactions applying the second-law and third-law methods.

The second-law method is based on the Van't Hoff equation and gives the standard enthalpy of reaction at the mid-range temperature $\langle T \rangle = 1/\langle T^{-1} \rangle$, as slope of the least-squares fitting of $\ln K$ vs. $1/T$:

$$\Delta_r H^\circ_{\langle T \rangle} = -R \frac{d(\ln K)}{d(1/T)} \quad (5a)$$

The enthalpy change at room temperature ($\Delta_r H^\circ_{298}$) can be calculated if heat capacities for all the species involved are known.

In the third-law method the $\Delta_r H^\circ_{298}$ is calculated at each experimental temperature by the relation:

$$\Delta_r H^\circ_{298} = -RT \ln K - T \Delta_r(G.e.f.)^\circ_T \quad (6a)$$

where $\Delta_r(G.e.f.)^\circ_T$ is the Gibbs energy functions change of the reaction. The $G.e.f.s$ for each species can be calculated if the heat capacities are known from 0 K to the experimental temperatures:

$$\begin{aligned} (G.e.f.)^\circ_T &= \frac{G^\circ_T - H^\circ_{298}}{T} \\ &= \frac{1}{T} \int_{298}^T C^\circ_p dT - \int_{298}^T \frac{C^\circ_p}{T} dT - S^\circ_{298} \end{aligned} \quad (7a)$$

Therefore the derivation of $\Delta_r H^\circ_{298}$ by both the second- and the third-law analyses of equilibrium data requires heat capacities data, although at a different extent. While the heat capacities were very recently [11,12] measured for all the calcium silicides between 3 and 300 K, apparently no data are available above room temperature. An approximation often employed is the Kopp–Neumann (KN) rule, i.e. the heat capacity of a compound is equal to the sum of the heat capacities of the constituent elements. However, the heat capacities and the absolute entropies obtained by applying this rule to calcium silicides at low temperatures are substantially lower (10% on average for absolute entropies) than the experimental ones for almost all the intermediate phases. Therefore the heat capacity values obtained with the additivity rule were scaled by a temperature-independent constant in order to eliminate the discontinuity with the experimental values at 298 K [11,12]:

$$C^\circ_{p,T} = C^\circ_{p,T}(KN) + [C^\circ_{p,298}(\text{exp}) - C^\circ_{p,298}(KN)] \quad (8a)$$

The $H^\circ_T - H^\circ_{298}$ and the high-temperature term of $G.e.f.$ were then calculated, while the S°_{298} values in Eq. (7a) were those given in [11,12]. The $G.e.f.$ values estimated for the calcium silicide phases are reported in Table 3. For sake of comparison, all the calculations were also performed assuming the Kopp–Neumann rule valid over the entire temperature range.

3.2. Enthalpy changes of decomposition reactions

Vaporization runs were performed on various alloy samples constituted of single phase stoichiometric compounds or mostly of two phases mixtures.

The decomposition equilibria studied were the following:

1. $\text{Ca}(\text{s}) = \text{Ca}(\text{g})$
2. $3\text{Ca}_2\text{Si} = \text{Ca}_5\text{Si}_3 + \text{Ca}(\text{g})$

3. $1/2\text{Ca}_5\text{Si}_3 = 3/2\text{CaSi} + \text{Ca(g)}$
4. $4\text{CaSi} = \text{Ca}_3\text{Si}_4 + \text{Ca(g)}$
5. $19/5\text{CaSi} = 1/5\text{Ca}_{14}\text{Si}_{19} + \text{Ca(g)}$
6. $\text{Ca}_3\text{Si}_4 = 2\text{CaSi}_2 + \text{Ca(g)}$
7. $2/9\text{Ca}_{14}\text{Si}_{19} = 19/9\text{CaSi}_2 + \text{Ca(g)}$
8. $\text{CaSi}_2 = 2\text{Si(s)} + \text{Ca(g)}$

The occurrence of these reactions was confirmed by XRD spectra performed on samples before and after vaporization. In particular we confirmed the high temperature decomposition of Ca_3Si_4 to $\text{Ca}_{14}\text{Si}_{19}$ in a 63at.% Si sample. This decomposition reaction occurs quickly, while the $\text{Ca}_{14}\text{Si}_{19}$ tends to remain as a metastable phase below the decomposition temperature.

A summary of the experimental features and the measured vapor pressure Eqs. $\log p_{\text{Ca}}/\text{bar} = -(A/T) + B$ is reported in Table 1 and in Figs. 2 and 3 as $\log p_{\text{Ca}}$ vs. $1/T$ plots for the Ca-rich and the Si-rich samples, respectively. In the same plots are also reported for comparison the few sets of calcium pressures measured previously by Wynnyckyj [4]. For easier comparison, these data were labelled by full markers with the same shape as our data points for samples of similar composition.

It has to be noted that in general our measurements, due to higher sensitivity of the techniques employed, extend to lower temperature and pressure ranges. In the case of Ca-rich alloys, namely for the two-phase region $\text{Ca}_5\text{Si}_3/\text{CaSi}$ (40.8at.% Si) the agreement is fairly satisfactory both in slope and in calcium pressure between ours and Wynnyckyj's [4] data. For the Si-rich alloys the pressure values we measured with two independent techniques appear somewhat higher than those reported by Wynnyckyj [4]. Furthermore the slope for the 51.4at.% Si alloy is considerably steeper compared with our result for reaction (5).

However, considering the high number of our data points and their reproducibility in different runs our results should be considered reliable and representative of equilibrium pressures over the two phase regions studied according to the phase diagram recently determined by Manfrinetti et al. [9].

The enthalpy changes for the vaporization reactions

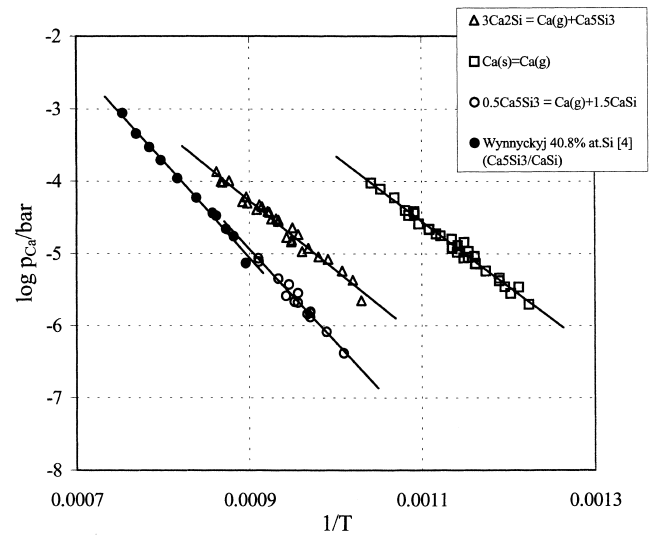


Fig. 2. $\log (p_{\text{Ca}}/\text{bar})$ vs. $1/T$ plot for the decomposition reactions of the Ca-rich phases in the Ca–Si system.

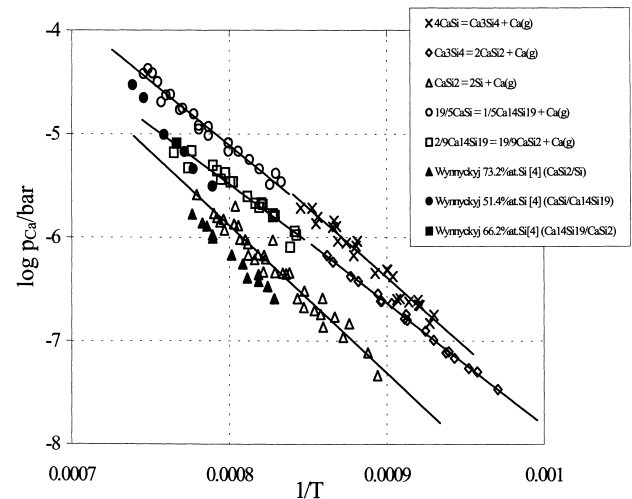


Fig. 3. $\log (p_{\text{Ca}}/\text{bar})$ vs. $1/T$ plot for the decomposition reactions of the Si-rich phases in the Ca–Si system.

which were derived from the second-law and third-law analysis of pressure–temperature data are presented in Table 2. For sake of comparison (and to demonstrate the

Table 1

Experimental conditions and measured vapor pressures for the decomposition reactions investigated

Reaction	Data points	Temperature range (K)	$\log p_{\text{Ca}}/\text{bar} = -A/T + B$	
			$A \cdot 10^{-3}$ (K)	B
$\text{Ca(s)} = \text{Ca(g)}$	31	817–960	9.026 ± 0.215	5.375 ± 0.244
$3\text{Ca}_2\text{Si} = \text{Ca}_5\text{Si}_3 + \text{Ca(g)}$	28	971–1160	9.594 ± 0.299	4.366 ± 0.279
$1/2\text{Ca}_5\text{Si}_3 = 3/2\text{CaSi} + \text{Ca(g)}$	15	990–1098	12.917 ± 0.615	6.688 ± 0.588
$4\text{CaSi} = \text{Ca}_3\text{Si}_4 + \text{Ca(g)}$	24	1075–1178	13.423 ± 0.542	5.694 ± 0.482
$19/5\text{CaSi} = 1/5\text{Ca}_{14}\text{Si}_{19} + \text{Ca(g)}$	22	1200–1341	12.377 ± 0.476	4.793 ± 0.373
$\text{Ca}_3\text{Si}_4 = 2\text{CaSi}_2 + \text{Ca(g)}$	19	1030–1160	11.837 ± 0.188	4.018 ± 0.144
$2/9\text{Ca}_{14}\text{Si}_{19} = 19/9\text{CaSi}_2 + \text{Ca(g)}$	20	1186–1298	11.219 ± 0.676	3.492 ± 0.547
$\text{CaSi}_2 = 2\text{Si(s)} + \text{Ca(g)}$	35	1118–1283	14.256 ± 0.554	5.516 ± 0.460

Table 2
Vaporization enthalpies for the intermediate phases of Ca–Si system

Reaction	$\Delta_r H^\circ_{(T)}$ II law kJ/mol	$\Delta_r H^\circ_{298}$ II law ^a kJ/mol	$\Delta_r H^\circ_{298}$ II law ^b kJ/mol	$\Delta_r H^\circ_{298}$ III law ^a kJ/mol (trend J/K)	$\Delta_r H^\circ_{298}$ III law ^b kJ/mol (trend J/K)
Ca(s) = Ca(g)	172.8 ± 1.8 at 880 K	178.3 ± 1.8	178.3 ± 1.8	180.6 ± 1.3 (3.2)	178.8 ± 1.2 (1.0)
3Ca ₂ Si = Ca ₅ Si ₃ + Ca(g)	183.6 ± 5.7 at 1066 K	240.6 ± 5.7	192.6 ± 5.7	111.7 ± 7.4 (–123.2)	211.0 ± 1.7 (17.1)
1/2Ca ₅ Si ₃ = 3/2CaSi + Ca(g)	247.2 ± 11.8 at 1046 K	250.5 ± 11.8	255.7 ± 11.8	241.7 ± 1.2 (–9.7)	227.4 ± 1.4 (–26.9)
4CaSi = Ca ₃ Si ₄ + Ca(g)	256.8 ± 10.4 at 1124 K	300.2 ± 10.4	267.0 ± 10.4	191.3 ± 7.3 (–142.7)	256.2 ± 1.5 (–13.1)
19/5CaSi = 1/5Ca ₁₄ Si ₁₉ + Ca(g)	236.9 ± 9.1 at 1275 K	253.1 ± 9.1	250.9 ± 9.1	265.4 ± 2.4 (10.9)	255.4 ± 2.5 (12.2)
Ca ₃ Si ₄ = 2CaSi ₂ + Ca(g)	226.5 ± 3.0 at 1094 K	235.1 ± 3.0	236.0 ± 3.0	261.3 ± 1.0 (23.1)	275.4 ± 1.3 (33.3)
2/9Ca ₁₄ Si ₁₉ = 19/9CaSi ₂ + Ca(g)	214.7 ± 12.9 at 1235 K	264.1 ± 12.9	227.7 ± 12.9	189.1 ± 2.4 (–82.3)	260.3 ± 0.7 (–10.6)
CaSi ₂ = 2Si(s) + Ca(g)	272.8 ± 4.6 at 1205 K	291.7 ± 4.6	285.1 ± 4.6	279.8 ± 4.0 (–0.1)	267.0 ± 2.5 (–21.9)

^a Calculated by means of thermal functions estimated correcting additive heat capacities according to the low temperature C_p° s of Canepa et al. [11,12] (see Eq. (8a)).

^b Calculated assuming additivity of the heat capacities (Neumann–Kopp rule).

influence of the uncertainties in the thermodynamic function estimates) we have reported $\Delta_r H^\circ_{298}$ values which were derived using different sets of thermodynamic functions ($H^\circ_T - H^\circ_{298}$ and $G.e.f.s$) calculated with different options as described previously in the text and in footnotes to Tables 2 and 3.

For some of the reactions studied the agreement between second-law and third-law $\Delta_r H^\circ_{298}$ is unsatisfactory. The difference in values is particularly striking in the case of reactions (2), (4), and (7) when the third-law values are calculated with the set of $G.e.f.$ functions estimated from the low temperature C_p° s and S°_{298} [11,12] (see Section 3.1). The agreement improves somewhat using the set of thermodynamic functions estimated with the additivity of the heat capacity in the entire temperature range. The discrepancy in the second-law and third-law $\Delta_r H^\circ_{298}$ parallels the anomalously large trend in the third-law

Table 3
Estimated Gibbs energy functions ($G^\circ_T - H^\circ_{298}$)/ T (J/K mol atoms) for the intermediate phases of the Ca–Si system^a

T/K	Ca ₂ Si	Ca ₅ Si ₃	CaSi	Ca ₃ Si ₄	Ca ₁₄ Si ₁₉	CaSi ₂
298 ^b	–40.8	–33.5	–34.1	–28.1	–34.5	–28.0
400	–42.8	–34.0	–35.8	–30.7	–35.9	–29.4
500	–45.4	–36.1	–38.1	–32.7	–38.2	–31.3
600	–48.4	–38.5	–40.8	–34.9	–40.9	–33.6
700	–51.5	–41.0	–43.5	–37.2	–43.7	–35.9
800	–54.5	–43.5	–46.2	–39.4	–46.4	–38.1
900	–57.5	–45.9	–48.8	–41.6	–49.0	–40.3
1000	–60.3	–48.2	–51.3	–43.8	–51.5	–42.4
1100	–62.6	–50.1	–53.4	–45.5	–53.6	–44.1

^a $G.e.f.s$ estimated by additive heat capacities corrected according to the low temperature C_p° s of Canepa et al. [11,12] (see Eq. (8a)).

^b ($G.e.f.$)_{298}^\circ = -S^\circ_{298}.}

$\Delta_r H^\circ_{298}$ values with temperature. For example in reaction (2) the Ca₂Si phase is involved for which the measured S°_{298} is much higher (20%), than the value calculated assuming additivity, compared to the other calcium silicides. As a consequence, and for sake of argument, the $G.e.f.$ values calculated at 900 K for Ca₅Si₃ using either complete additivity or the low-temperature C_p° s differ by 2 J/K mol atoms (or 4%) while the difference for Ca₂Si amounts to 12 J/K mol atoms (or 19%). The uncertainty in the calculated $G.e.f.$ values is ultimately reflected in the third-law values of $\Delta_r H^\circ_{298}$. Incidentally, we note that the entropies of formation of calcium silicides calculated from experimental heat capacities [11,12] are positive or slightly negative while, in contrast, the few earlier data indicate strikingly large negative values [6,7]. Measurements of heat capacities at high temperature for the pure calcium silicide phases would be necessary to improve the calculation of the thermodynamic functions, in primis of the Gibbs energy functions. As we have no indication of gross errors in temperature and vapor pressure measurements we assume that a major role may be played in the observed discrepancy between second-law and third-law results by inaccuracies in the heat contents and Gibbs energy functions used in the analysis.

The slopes of $\ln K$ vs. $1/T$ curves are not affected by possible inaccuracies in the value of the instrumental constant k_{str} while this is the case of the third-law results. In view of this fact and the large number of pressure data points and the reproducibility of data in the various vaporization experiments, we believe that the second-law values are more reliable for all the studied decomposition reactions.

3.3. Heats of formation of calcium silicides

The decomposition enthalpies $\Delta_r H^\circ_{298}$ presented in column 3 of Table 2 enable us to calculate the standard enthalpies of formation of the solid calcium silicides. The heat of formation of CaSi_2 was simply calculated by subtracting the standard vaporization enthalpy of pure calcium ($\Delta_{\text{sub}} H^\circ_{298}(\text{Ca}) = 178.2 \text{ kJ/mol}$ [13]) from $\Delta_r H^\circ_{298}$ for reaction (8). Incidentally, in a vaporization experiment of pure Ca(s) we found a $\Delta_{\text{sub}} H^\circ_{298}(\text{Ca})$ practically coincident with the assessed value [13]. Thereafter values for all the intermediate phases were derived from reactions (7) to (2). Due to the presence of two different vaporization equilibria involving the CaSi decomposition (equilibria (4) and (5)), our experimental $\Delta_r H^\circ_{298}$ data exceed the unknowns to be calculated. In other words, two different $\Delta_r H^\circ_{298}$ for CaSi may be derived from reactions (4) and (5), respectively. However both values are in close agreement: -50.7 ± 1.8 and $-48.4 \pm 2.6 \text{ kJ/mol atoms}$, indicating the self-consistency of the data. For this reason we propose for the heat of formation of CaSi the average of the two results. This value has also been used to calculate the $\Delta_r H^\circ_{298}$ for Ca_5Si_3 and Ca_2Si . The enthalpies of formation are presented in the last column of Table 4 and in Fig. 4.

Our values can be compared with literature data for Ca_2Si , CaSi and CaSi_2 ; for the other phases Ca_5Si_3 , Ca_3Si_4 and $\text{Ca}_{14}\text{Si}_{19}$, they represent first determinations. The results reported many years ago from Kubaschewski and Villa [2] are practically the only published calorimetric data of the formation enthalpies of calcium silicides. These authors carried out adiabatic calorimetry measurements on a number of Ca-Si alloys and then derived $\Delta_r H^\circ_{940}$ for the three phases known at the time. Previous calorimetric results from Schneider and Stobbe (private communication in Ref. [2]) were therein criticized and the value subsequently determined for the Ca_2Si phase ($\Delta_r H^\circ_{298} = -161.8 \text{ kJ/mol atoms}$) seems unreasonably negative [3]. The Kubaschewski and Villa's results are reported in Table 4,

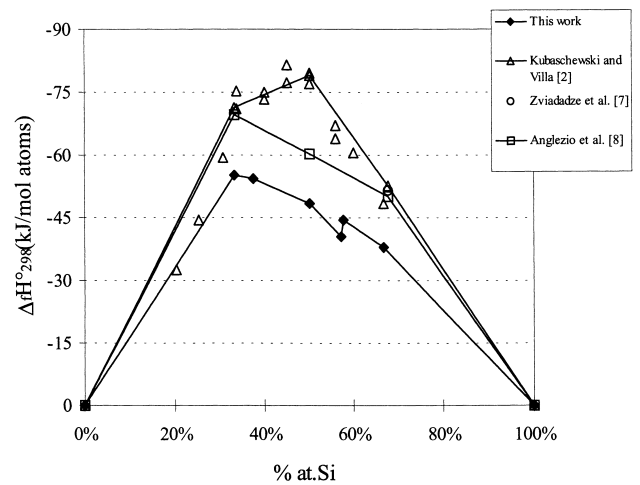


Fig. 4. Heats of formation at 298 K for the calcium silicides.

along with the only electrochemical data [7] and the values derived by phase diagram optimization [8]. Table 4 and Fig. 4 reveal that the $\Delta_r H^\circ_{298}$ we derived are quite lower than the calorimetric data [2]. Wynnyckyj and Pidgeon [4] came to a similar conclusion from their activity data. Though they did not derive any numerical data for the heats of formation of calcium silicides, they stated that ‘the calorimetric values [of Kubaschewski and Villa] are substantially higher than the present ones’. Indeed, the heats of formation derived in Ref. [8] from the Wynnyckyj’s data ($\Delta_r H^\circ_{298}(\text{CaSi}) = -46.0 \text{ kJ/mol atoms}$ and $\Delta_r H^\circ_{298}(\text{CaSi}_2) = -36.7 \text{ kJ/mol atoms}$) are in excellent agreement with our results. On the other hand, the electrochemical value for CaSi_2 is very close to the calorimetric value. Another feature of our $\Delta_r H^\circ_{298}$ is that the maximum is obtained for the phase Ca_2Si whose melting point is 50°C lower than that of CaSi . This results apparently confirm the findings from the phase diagram optimization (Table 4).

The influence of the estimated heat contents of the compounds on $\Delta_r H^\circ_{298}$ should be emphasized. For exam-

Table 4

Comparison between standard heats of formation (kJ/mol atoms, $T=298 \text{ K}$) of Ca-Si intermediate phases from literature and present work

Phase	Kubaschewski and Villa (calorimetry) [2]	Zviadadze and Kereselidze (emf) [7]	Anglezio et al. (phase diagram assessment) [8]	This work ^a
Ca_2Si	-71.4 ± 4.2 (at $T=940 \text{ K}$)		-69.7	-56.1 ± 3.1
Ca_5Si_3				-55.3 ± 3.5
CaSi	-79.1 ± 4.2 (at $T=940 \text{ K}$)		-60.3	-49.6 ± 2.2^b
Ca_3Si_4				-40.6 ± 1.5
$\text{Ca}_{14}\text{Si}_{19}$				-44.4 ± 2.3
CaSi_2	-52.7 ± 2.5 (at $T=940 \text{ K}$)	-51.5	-50.1	-37.8 ± 1.6

^a Calculated assuming $\Delta_r H^\circ_{298}$ reported in the column 3 of the Table 2.

^b Average value calculated from reactions (4) and (5) (see text).

ple, adopting the additivity of C_p° would result in heat of formation values fairly lower (by up to 15% for the phase Ca_2Si), with the phase Ca_5Si_3 having the most negative $\Delta_f H_{298}^\circ$ (-51.0 kJ/mol atoms). In order to display the potential effects of the inaccuracies in heat content estimates, we also calculated the heats of formation at $T = 1100$ K for all phases. This temperature is approximately the mid-range temperature of our experiments. Therefore these values are only weakly affected by the heat contents. At this temperature the most stable phase is Ca_5Si_3 ($\Delta_f H_{298}^\circ = -53.0$ kJ/mol atoms), followed by Ca_2Si ($\Delta_f H_{298}^\circ = -48.5$ kJ/mol atoms) and CaSi ($\Delta_f H_{298}^\circ = -44.5$ kJ/mol atoms).

To conclude, in order to definitely set the thermochemistry of the calcium–silicon system, we would suggest further accurate calorimetric determination of the heats of formation of all the calcium silicides phases and the measurement of the heat capacities at high temperature.

Acknowledgements

The planning and development of the studies here presented form a part of an Italian National Research Project entitled ‘Leghe e Composti Intermetallici: stabilità termodinamica, proprietà fisiche e reattività’. The authors would like to thank the Ministero per la Ricerca Scientifica e Tecnologica (Programmi di rilevante interesse tecnologico) for their financial support. This work was also partially supported by CNR–Centro di Termodinamica

Chimica alle Alte Temperature and Università di Roma ‘La Sapienza’.

Thanks are also due to Mr. P. Trionfetti for carrying out thermogravimetric experiments and to Mr. G. Minelli of the CNR–SACSO for checking by XRD some vaporization residues.

References

- [1] T.B. Massalski, P.R. Subramanian, H. Okamoto, L. Kacprzak, Binary Alloy Phase Diagrams, 2nd Edition, ASM International, Material Park (OH), 1990.
- [2] O. Kubaschewski, H. Villa, Z. Elektrochem. 53 (1949) 32.
- [3] S.A. Shchukarev, M.P. Morozova, G.F. Pron, Zh. Obshch. Khim. 32 (1962) 2069.
- [4] J.R. Wynnycyk, High Temp. Sci. 4 (1972) 205.
- [5] J.R. Wynnycyk, L.M. Pidgeon, Met. Trans. 2 (1971) 975.
- [6] V.G. Muradov, P.V. Gel'd, P.V. Kocherov, Russ. J. Phys. Chem. 41 (1967) 5.
- [7] G.N. Zviadadze, M.V. Kereselidze, Tr. Inst. Met. Akad. Nauk. Gruz. SSR 15 (1966) 88.
- [8] J.C. Anglezio, C. Servant, I. Ansara, CALPHAD 3 (1994) 273.
- [9] P. Manfrinetti, M.L. Fornasini, A. Palenzona, Intermetallics 8 (2000) 223.
- [10] M. Affronte, O. Laborde, G.L. Olcese, A. Palenzona, J. Alloys Comp. 274 (1998) 68.
- [11] F. Canepa, M. Napoletano, P. Manfrinetti, A. Palenzona, J. Alloys Comp. 299 (2000) 20.
- [12] F. Canepa et al., to be published.
- [13] R. Hultgren, P.J. Desai, D.T. Hawkins et al., Selected Values of Thermodynamic Properties of the Elements, American Society of Metals International, Metals Park, OH, 1973.